

Use of Statistical Analysis of Acoustic Emission Data on Carbon-Epoxy COPV Materials-of-Construction for Enhanced Felicity Ratio Onset Determination

Arick Reed A. Abraham,¹ Kenneth L. Johnson,² Charles T. Nichols,³ Regor L. Saulsberry,³ and Jess M. Waller⁴
NASA-JSC White Sands Test Facility, 12600 NASA Rd., Las Cruces, NM, 88012

Broadband modal acoustic emission (AE) data were acquired during intermittent load hold tensile test profiles on Toray T1000G carbon fiber-reinforced epoxy (C/Ep) single tow specimens. A novel trend seeking statistical method to determine the onset of significant AE was developed, resulting in more linear decreases in the Felicity ratio (*FR*) with load, potentially leading to more accurate failure prediction. The method developed uses an exponentially weighted moving average (EWMA) control chart. Comparison of the EWMA with previously used *FR* onset methods, namely the discrete (*n*), mean (\bar{n}), normalized (*n*%) and normalized mean (\bar{n} %) methods, revealed the EWMA method yields more consistently linear *FR* versus load relationships between specimens. Other findings include a correlation between AE data richness and *FR* linearity based on the *FR* methods discussed in this paper, and evidence of premature failure at lower than expected loads. Application of the EWMA method should be extended to other composite materials and, eventually, composite components such as composite overwrapped pressure vessels. Furthermore, future experiments should attempt to uncover the factors responsible for “infant mortality” in C/Ep strands.

Nomenclature

AE	=	acoustic emission
ASTM	=	American Society for Testing and Materials
C/Ep	=	carbon-fiber impregnated with epoxy
COPV	=	composite overwrapped pressure vessel
DWC	=	Digital Wave Corporation
EWMA	=	exponentially weighted moving average
FFT	=	fast Fourier transform
<i>FR</i>	=	Felicity ratio
<i>FR</i> *	=	extrapolated Felicity ratio at rupture (strand) or burst (COPV)
ILH	=	intermittent load hold
<i>LR</i>	=	load ratio
NDE	=	nondestructive evaluation
<i>n</i> %	=	the first <i>n</i> percent of AE events used to calculate the Felicity ratio
<i>n</i>	=	the first <i>n</i> AE events used to calculate the Felicity ratio
\bar{n} %	=	the mean of the first <i>n</i> percent of AE events used to calculate the Felicity ratio
\bar{n}	=	the mean of the first <i>n</i> AE events used to calculate the Felicity ratio
<i>R</i> ²	=	linear least squares coefficient of determination
SHM	=	structural health monitoring
UTS	=	ultimate tensile strength

¹ USRP Intern, Kate Gleason College of Engineering, Rochester Institute of Technology, Rochester, New York 14623.

² Statistician, NASA/NESC Systems Engineering Office, MSFC, AL 35812.

³ Project Managers, NASA-JSC White Sands Test Facility, Laboratories Department, MS 200LD, Las Cruces, New Mexico 88004.

⁴ Materials Scientist, NASA-JSC White Sands Test Facility, Laboratories Department, MS 200LD, Las Cruces, New Mexico 88004.

I. Introduction

Aerospace companies and agencies including the National Aeronautics and Space Administration (NASA) are increasingly relying on polymer matrix composite materials in launch vehicles, satellites, and aircraft in order to save weight and increase payload. High performance polymer matrix composites have higher specific strengths than their metallic counterparts, further increasing their proliferation in load-bearing applications. The increasing use of composite materials in aerospace applications, remove-and-inspect considerations, and the accessibility of test articles have all put great emphasis on developing nondestructive structural health monitoring (SHM) methods. Despite widespread and increasing use, relatively few nondestructive evaluation (NDE) SHM techniques have been developed. Visual methods often detect little to no change in a composite until the material fractures. Techniques in development for characterization of composite overwrapped pressure vessels (COPVs) include eddy current scanning, laser shearography and profilometry, acoustic emission (AE), dielectric impedance, and dye penetrant inspection. Compared to these methods, AE is especially well-suited for characterization of composites^{1,2,3,4} and COPVs.⁵

NASA has a vested interest in the use of COPVs on launch vehicles and satellites. COPVs consist of a thin metal liner typically wrapped in aramid or carbon fiber embedded in a matrix of thermosetting polymer, typically an epoxy. The liner holds the storage media and is generally load sharing, while the epoxy transfers stress from the liner to the fiber and bears the majority of the load in the COPV. NASA systems incorporating COPVs include the International Space Station, Space Shuttle, Space Launch System and Orion Crew Capsule. Other systems include essentially every satellite in use. Stress ruptures of the composite overwrap in a COPV are especially concerning; they can lead to a catastrophic ‘burst before leak’ failure event which occurs with little to no warning. Some of the visual indicators preceding burst include tow breakage or excessive matrix cracking. These visual indicators only suggest impending failure, and cannot be used to pinpoint the failure pressure.

NASA White Sands Test Facility (WSTF) has worked to develop and refine AE monitoring as an NDE and SHM technique for COPVs. AE is a passive technique, which differentiates it from other NDE and SHM techniques. AE monitoring measures a structure's real-time response to applied stress instead of interpreting the response of signals actively sent into a structure. Although more costly to develop than other NDE techniques, AE monitoring shows promise for post-manufacture qualification, in-service inspection, and in-situ SHM. Once developed, AE monitoring has the potential to dramatically reduce the mission critical or life-threatening risks associated with the use of composites.

Because AE monitoring as an SHM technique for COPVs currently is in infancy, testing focuses on monitoring inexpensive uniaxial, single tow specimens subjected to tensile loading. Uniaxial tensile testing offers a simple and well-known platform to refine the test system's configuration and identify the trends that can be used to interpret AE data.

II. Background

A. Stress Waves

A material placed under load will deform, resulting in the creation and growth of flaw sites. This process releases energy through transient elastic stress waves, called acoustic emissions, which propagate to the surface of the material and are detected as AE events. A sensor array detects and records these events for processing and analysis.

B. Failure Prediction Using Felicity Ratios

The methodology for failure prediction with AE varies, including modeling the energy release rate⁶ or qualitatively monitoring the AE event rate for sudden increases.⁷ The WSTF approach uses the Kaiser effect, which states a structure will only release significant AE when exposed to applied stresses higher than previously encountered.⁸ Certain conditions lead to a violation of the Kaiser effect, known as the Felicity effect, quantitatively measured using the Felicity ratio (FR) (Eq. 1). Kaiser effect violations demarcate the occurrence of critical micromechanical damage and indicate impending failure (Eq. 1). Previous results show a linear fit (Eq. 3) can accurately model the dependence of FR plotted versus the load ratio (Eq. 2).^{9, 10, 11, 12}

$$FR = \frac{\text{Load at Onset of Significant AE}}{\text{Load at Previous Load Hold}} \quad (1)$$

$$LR = \frac{\text{Load at Felicity Ratio Calculation}}{\text{Load at Sample Failure}} \quad (2)$$

$$FR = (m \times \text{load}) + b \quad (3)$$

An intermittent load-hold (ILH) stress schedule can be used to excite the tensile specimen for AE testing (see Section III.B) by exposing a specimen to incrementally increasing load holds. Compared to single-cycle tensile tests (for example, a proof cycle), this allows for the collection of more *FR* data points per specimen.¹³ *FR*-based failure predictions (Eq. 4) rely on assuming *FR* linear dependence on load ratio (*LR*) (Eq. 3), which allows use of the *FR* behavior of a sample population to predict the behavior of an individual specimen. The *FR* behavior for a population of like specimens (FR_{pop}^*) averages each specimen's *FR* at failure (FR^*). Prediction assumes unknown specimens of the test population will fail following a similar *FR*-behavior.

$$\text{Predicted Failure Load} = \frac{FR_{pop}^* - b}{m} \quad (4)$$

C. Onset of Significant Acoustic Emission

FR-based failure prediction highly depends on the method used to determine the onset of significant AE. Previous WSTF research defined the onset of significant AE in one of several ways: a) as a discrete AE event occurring in a load ramp (*n* method); b) as the event occurring at a normalized percentage of the total number of AE events into the load ramp (*n*% method); or c) and d) as the averages of the discrete or normalized onset of significant AE (\bar{n} and \bar{n} % methods) (Figure 1).¹²

These “n-methods” have proven useful in optimizing the *FR* vs. *LR* linear fit; however, the best n-method varied from specimen to specimen, or material to material.¹² For example, the \bar{n} method successfully determined the onset for HexTow^{®1} IM7 strands, while the normalized *n*% method successfully determined the onset for Toray T1000G strands. Specimen-to-specimen scatter, type of AE equipment, AE data acquisition parameter settings, sensor type, and sensor configuration add further inconsistency to *n*-method results.

¹ HexTow[®] is a registered trademark of Hexcel Corporation, Dublin, California.

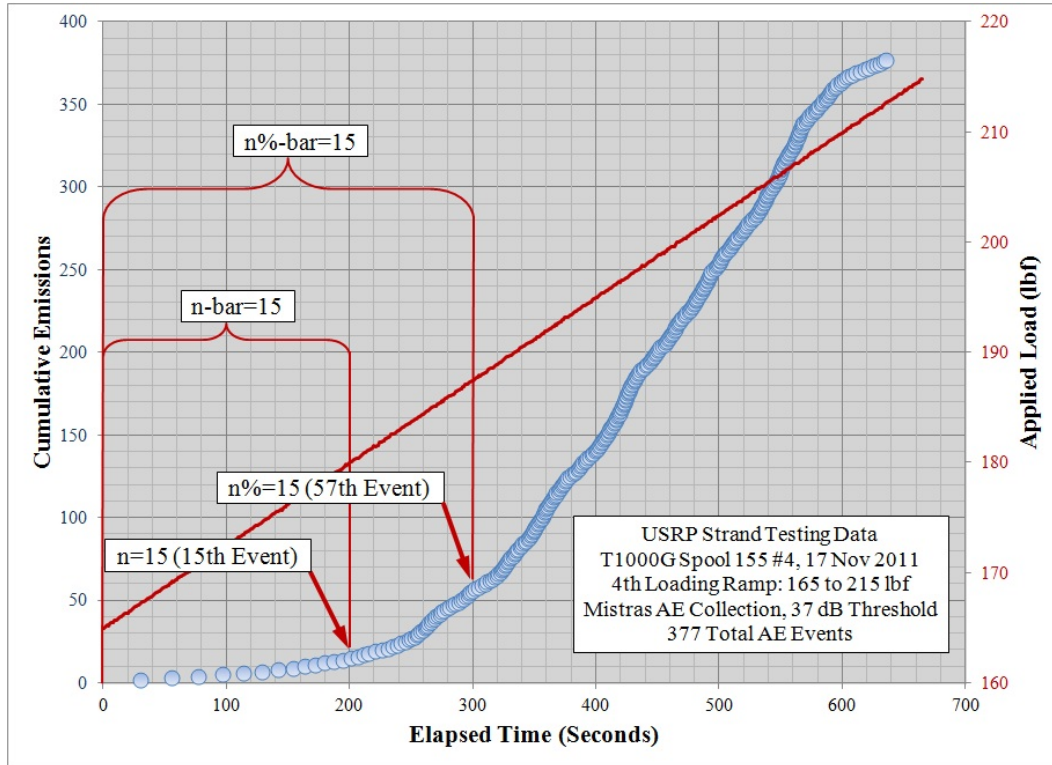


Figure 1. Onset method overview. *Location of the onset as determined by various n -methods.*

D. Development of the Exponentially Weighted Moving Average

Quantitative failure prediction techniques using FR are scarce. American Society for Testing and Materials (ASTM) standards offer separate onset determination guidelines.^{7, 13, 14} An ASTM addendum introduces the *knee in the curve* (Figure 2) as onset criteria, defined as “a dramatic change in the slope of the cumulative AE versus time curve.”¹⁴ The ‘knee method’ remains problematic because the definition is subjective. The desire to overcome these issues led to the goal of this study: to create a more accurate, quantitative, and consistent method for determining the onset of significant AE events than is presently available in consensus methods^{7, 13, 14} and previous NASA research.¹² This goal led to the development of the exponentially weighted moving average (EWMA), discussed below. Together, it is hoped the n -method and EMWA method will encompass most or all expected FR -behavior for carbon fiber-reinforced epoxy (C/Ep) and other polymeric matrix composites, allowing powerful analysis tools to ascertain the real-time health of composite materials and structures.

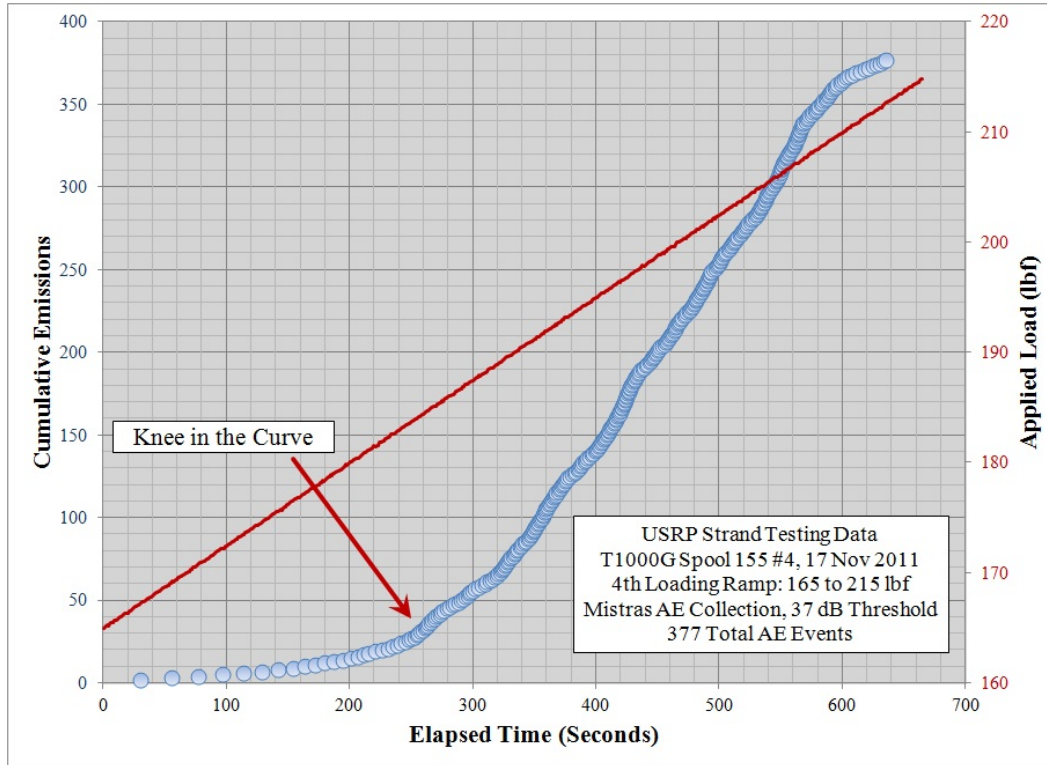


Figure 2. “Knee” overview. Location of the onset as determined by a “knee in the curve.”

E. Emphasis on Least Residuals

It is very important to note that the FR^*_{pop} of a population of strands depends on the chosen onset determination method. *A priori*, no universal onset determination method or FR^*_{pop} exists which can predict the behavior of a series of specimens of the same or different material type. Predicted failure load depends on FR^*_{pop} , making it an unreliable quantity without a proven, consistent onset method. What is sought is not an onset determination method that gives the best linear fit for a given specimen, but one that consistently gives the best fit across the entire population. Therefore, this study emphasizes finding a method that gives consistently good prediction across the entire population which can lead to reliable predicted failure loads.

III. Experimental

The uniaxial tow specimens tested were 3817-denier Torayca^{®1} T1000G carbon fiber strands (Table 1) from Toray Carbon Fibers America, Inc. (Santa Ana, California), impregnated in a proprietary 121 °C (250 °F) epoxy matrix. The published fiber volume fraction of the strand is 0.60.¹⁹

Table 1. Strand properties: 3817-denier Torayca T1000G

Filament Count	Tensile Strength	Geometry	Cross-section Area	Nominal Thickness	Nominal Width
12,000	1268 ± 307 N (285 ± 69 lbf) ¹²	Ribbonlike	0.236 mm ² (0.365 mil ²) ¹²	0.36 mm (0.014 in.) ¹²	1.4 mm (0.057 in.) ¹²

¹ Torayca[®] is a registered trademark of Toray Industries, Inc., Tokyo, Japan.

A. Specimen Preparation

Specimen preparation was based on ASTM standards,^{15, 16} comprising a 10-in. uniaxial tow specimen anchored on each end with epoxy to cardboard tabs.¹¹ Previous experiments at WSTF optimized the procedure to maximize the probability of a gauge-region fracture resulting from tensile stress.^{9, 10, 11, 12} Modifications used in this study included incorporating longer tabs measuring 2.5 in. long by 1 in. wide. This change lessens the odds of grip failure by directing stress further into the gauge region. Hardman^{®1} 1:1 Extra Fast Setting Epoxy (Table 2) bonds the strand and tabs and was given at least a 24-hour cure time.¹⁷

Table 2. Properties of 1:1 Hardman Extra-Fast Setting Epoxy

Package	Volume	Shear Strength (1 hr cure)	Shear Strength (24 hr cure)	Working Time	Handling Time
Red #04001	3.4 g (0.12 oz.)	10 MPa (1500 psi)	20 MPa (3000 psi)	3 min	15 - 30 min

B. Tensile Tests

Testing was performed with an Instron^{®2} Model 5569 electromechanical test instrument outfitted with a 50 kN (11,200 lb_f) load cell and Instron Bluehill software (version 1.8.289). Calibration was performed prior to each test. Self-tightening 25 × 50 mm (1 × 2 in.) wedge action grips with knurled faces held the specimens. The ILH tensile test profile is described in Table 3.

Table 3. Intermittent Load Hold Stress Schedule

ILH Method for Tensile Tests	
1.	Hold 30 min at nominal 20 N (5 lb _f) preload
2.	Ramp: Load to 534 N (120 lb _f)
3.	Hold at constant load: 10 min
4.	Ramp: Unload 89 N (20 lb _f)
5.	Hold at constant load: 10 min
6.	Ramp: Load 222 N (50 lb _f)
7.	Repeat Steps 3-5 until ultimate tensile strength (UTS) reached

C. Acoustic Emission Monitoring Equipment

Two AE monitoring systems were used: a Digital Wave Corporation (DWC, Centennial, Colorado) 8-channel 16-bit FM-1 system and a Mistras^{®3} Group, Inc. 8-channel 18-bit PCI-2 system.

The DWC FM-1 system was capable of recording AE events sympathetically with frequencies up to 20 MHz. Tests used 4 channels connected to DWC model PA-0 preamplifiers with 0 dB gain and DWC Model B1080 broadband, high fidelity piezoelectric sensors with a 50 kHz to 2.0 MHz range. Sensor and preamplifier consistency was maintained between tests barring hardware failure. DWC Wave Explorer (version 6.2.0) recorded AE data to a “lunchbox” computer system. Two configurations were used for the DWC FM-1 signal conditioner and triggering unit (Table 4). Wavelet amplitude thresholds were set as sensitive as possible at all times, and test variables occasionally necessitated the less sensitive 43 dB threshold (configuration DWC-B). Decibels are referenced against one microvolt in the DWC FM-1 system with a triggering threshold of 100 mV.

¹ Hardman[®] is a registered trademark of Elementis Performance Polymers, Belleville, New Jersey.

² Instron[®] is a registered trademark of Instron Corporation, Canton, Massachusetts.

³ Mistras[®] is a registered trademark of MISTRAS Group, Inc., Princeton Junction, New Jersey.

Table 4. Digital Wave Corporation FM-1 settings & estimated resulting thresholds.

System Configuration	Preamp Gain, x6 dB	Signal Gain, dB	Signal HP Filter, kHz	Trigger Gain, x3 dB	Trigger Gain, dB	Trigger HP Filter, kHz	Trigger LP Filter, MHz	Resulting Threshold, dB
DWC-A	5	24	20	2	20	50	1.5	40
DWC-B	5	24	20	1	20	50	1.5	43

The Mistras Group, Inc. PCI-2 system is capable of recording AE hits independently with frequencies up to 10 MHz. Tests used two channels connected to Mistras Model 2/4/6 preamplifiers capable of 0, 20, or 40 dB gain and Mistras Model WD broadband, high fidelity piezoelectric sensors with a 100 to 900 kHz range. Sensor and preamplifier consistency was maintained between tests. The PAC Windows Platform of PACwin Suite (version E4.50) included AEwin™ and AEwinPost™, and recorded AE data to the integrated computer in the PCI-2 system. Various configurations of AE collection parameters (Tables 5 and 6) generated different thresholds. No precedent existed in WSTF experiments for Mistras AE system use during carbon fiber strand testing. The various thresholds indicate efforts to put the threshold as low as possible, making the system as sensitive as possible, without detecting a constant stream of electronic noise.

Lord^{®1} 202 acrylic adhesive and Lord 17 accelerant were used to bond sensors to the strand at a 10:1 ratio equidistantly from each other and the gauge region.

Table 5. Mistras Group AE collection waveform settings.

Wavelet Sampling Rate, MSPS or MHz	Pre-Trigger Points, points/wave	Wavelet Length, points/wave	Peak Definition Time, μ s	Hit Definition Time, μ s	Hit Lockout Time, μ s	Maximum Duration, μ s
5	256	9000	200	800	1000	100

Table 6. Mistras Group AE collection parameters.

System Configuration	Low Pass Filter, kHz	High Pass Filter, MHz	Threshold Type	System Gain, dB	Preamplifier Gain, dB	Threshold, dB
Mistras-A	100	1	Fixed	0	20	37
Mistras-B	100	1	Fixed	0	20	38
Mistras-C	100	1	Fixed	0	20	39
Mistras-D	100	1	Fixed	0	20	40
Mistras-E	100	1	Fixed	0	20	46

IV. Results & Discussion

A. Data Filtering

More sensitive AE data acquisition settings (lower thresholds, approximately 37 dB for Mistras or 40 dB for DWC) collect more data but can increase the amount of recorded noise. Distinguishing between noise and genuine events is problematic with data collected by the DWC system. Threshold and frequency based filters are ineffective for low energy events. Each waveform is inspected and qualitatively validated. Noise will appear as an instantaneous spike in voltage followed by negligible voltage over time. The Fast Fourier Transform (FFT) may show frequencies unassociated with micromechanical damage.² Events caused by noise and low-energy AE events are easily confused, making filtering problematic. Therefore, DWC AE data are not filtered for noise, which could affect accuracy as these emissions skew the *FR* onset points.

Mistras AE data contain more information about individual hits with suitable filtering criteria, specifically the duration and peak frequency of the AE event. A duration of 0 ms suggests either the wave touched (not crossed) the

¹ Lord[®] is a registered trademark of Lord Corporation, Cary, North Carolina.

threshold or the event happened instantaneously. Inspection of the individual waveform points to these events as indicative of noise. Alternatively, a peak frequency of 4 kHz was noted in this study, which is outside of the 100 - 900 kHz bandwidth of the WD sensors. Since 4 kHz is within the audible frequency band, this was considered to be noise. Furthermore, 4 kHz is far below what any study has observed as a frequency associated with micromechanical damage in carbon-fiber composites.² Therefore, filtering eliminated AE events with 0-ms durations and/or 4 kHz peak frequencies.

B. Exponentially Weighted Moving Average

The exponentially weighted moving average (EWMA) control chart is used in statistical quality control. It consists of a plotted statistic with a built-in smoothing function and a set of control limits. The EWMA chart, recommended by statistician Kenneth Johnson of the NASA / NESC Systems Engineering Office, shows potential for consistent location of the ‘knee’ corresponding to the onset of significant AE for *FR* determination. The chart monitors the plotted statistic (Eq. 5) for trend changes. For onset determination, it is the time after the start of a loading ramp for each AE event occurrence. A smoothing constant prevents “noisy” data from erroneously indicating a new trend.

$$z_i = \lambda x_i + (1 - \lambda)z_{i-1} \quad (5)$$

The plotted statistic (z_i) is a summation of previous plotted statistics. Initially, z equals the first observation value times the smoothing constant (λ). The previous plotted statistic (z_{i-1}) equals the plotted statistic (z_i) of the prior iteration. The smoothing constant (λ) represents the percentage of weight given to the current observation’s influence on the plotted statistic. In this application, the current observation (x_i) equals the time of the AE hit at the current iteration.

Control limits (Eq. 6) act as alarms. Inside their boundaries, the plotted statistic’s trend is changing; outside the boundaries, the plotted statistic is following a trend.

$$Limits = T \pm L \frac{S}{\sqrt{n}} \sqrt{\frac{\lambda}{2 - \lambda} [1 - (1 - \lambda)^{2i}]} \quad (6)$$

The average of unsmoothed data to the current iteration (T) in this application adds all AE event times, including the current iteration’s event time, divided by the total number of AE events. The number of standard deviations away from the mean (L) determines the sensitivity of trend detection. A moving range determines the theoretic standard deviation (S) (Eq. 7). The rational subgroup size (n) indicates the number of data points in a single observation, equaling 1 in this application. The smoothing constant (λ) equals its value in the plotted statistic equation (Eq. 5). The observation count (i) equals the current observation number of the plotted statistic (z_i).

$$S = \hat{\sigma} = \frac{\sum_{i=0}^i MR_i}{(i - 1)d_2(2)} \quad (7)$$

The moving range (MR_i) is the current observation minus the previous observation, in this instance the current AE hit time minus the previous AE hit time. The observation count (i) equals its value in the control limit equation (Eq. 6). The unbiasing constant (d_2) equals 1.128 for a moving range of 2.¹⁸ The smoothing constant (λ) is equivalent to its value and meaning in the plotted statistic equation (Eq. 5); it represents the percentage of weight the current event will influence the limits.

This study used a smoothing constant (λ) of 0.17 and an allowable standard deviation (L) of 2.8. These values could change for other composite materials and structures. The constant values listed for each equation have proven effective for T1000G strand tests regardless of the type AE equipment or threshold used. Both λ and L are initially set within a range recommended by a statistician for the application at hand, and the values adjusted experimentally to produce the best results.

To determine the onset of significant AE for *FR*, a loading ramp is segmented into three time zones (Fig. 3). Zone 1 comes before the ‘knee,’ zone 2 marks the transition around the ‘knee’ between the control limits, and zone 3 comes after the ‘knee.’ The first AE event in zone 3 defines the onset of significant emissions for *FR* determination. Note the EWMA method can detect the change in trend before it is visually detected as a ‘knee.’

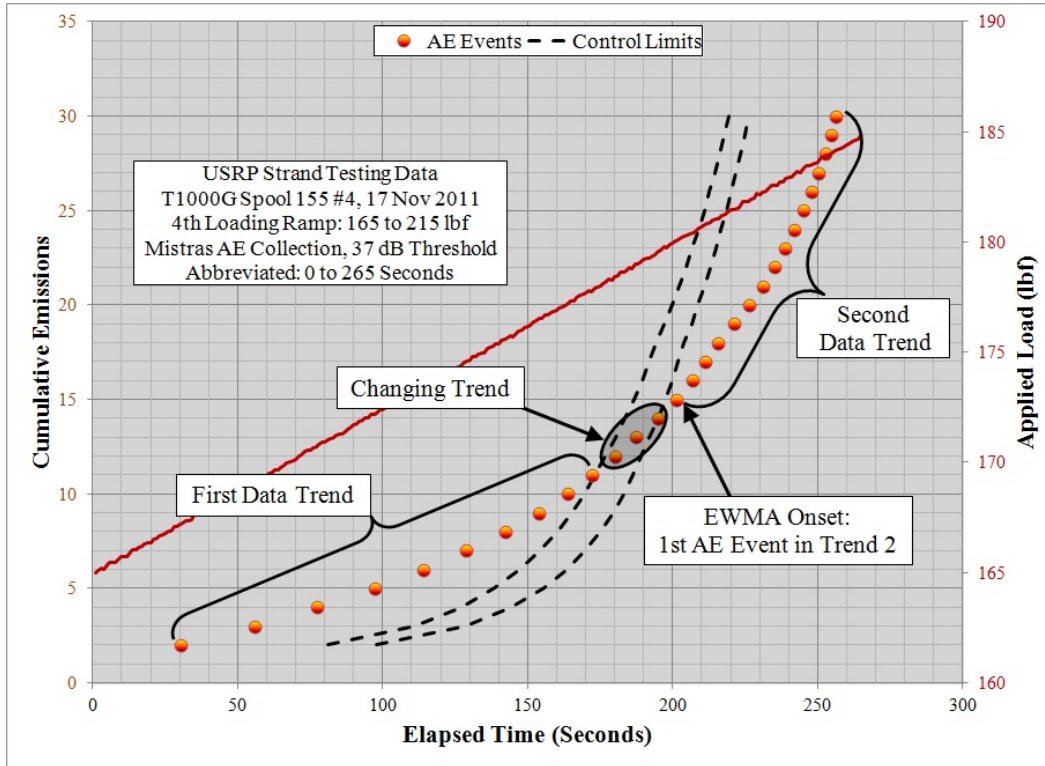


Figure 3. Exponentially weighted moving average example region. Cumulative AE events versus time curve, focusing on region of changing trend by EWMA method with the onset labeled.

C. Comparison of Analysis Methods

Comparative analysis consisted of applying each *n*-method with *n* or *n*% equaling 5 through 25 in increments of 5 and the EWMA method. A linear regression was fitted to the resulting *FR* data points, specifically noting the correlation coefficient (R^2) of each fit. A desirable method would have consistently high agreement between data points resulting in a high average R^2 value and a low standard deviation for the method’s application across the entire population.

D. General Results Discussion

Out of 20 T1000G strands tested, 15 yielded acceptable results (Table 7). Reasons for omitting tests included lack of AE data (due to equipment failure or user error) or undesirable failure modes (failures resulting in pull-out from grip or fracture in the grip). Tests with AE events numbering higher than 10,000 were possible by using the higher-sensitivity system at the lowest possible threshold (Section IV.A) which generated the richest populations of data. Strand S104#2 is notable for its valid failure at the lowest load of the population, which could have implications regarding “infant mortality” (Section IV.H).

The collection of all linear *FR* versus *LR* trend lines converge towards FR^*_{pop} as *LR* approaches 1 (Fig. 4). The EWMA2 method (Section IV.G) offers the tightest convergence, which could still be improved by more sensitive (Section IV.E) AE data acquisition settings.

Table 7: General results of T1000G strand testing.

Date	Sample ¹	AE System	Threshold (dB)	AE Events	Load at Failure (lb _f)
17 Oct 2011	S033 #1	DWC	43	544	275 ²
18 Nov 2011	S074 #2	Mistras	39	1557	325
29 Sep 2011	S104 #1	DWC	40	4557	325
08 Nov 2011	S104 #2	Mistras	40	2690	240 ²
13 Oct 2011	S140 #1	DWC	43	2726	305
29 Nov 2011	S140 #2	Mistras	37	14397	328
06 Oct 2011	S155 #2	DWC	40	2878	305
07 Oct 2011	S155 #3	DWC	40	4863	305
17 Nov 2011	S155 #4	Mistras	37	16294	365
11 Oct 2011	S169 #1	Mistras	46	504	291
16 Nov 2011	S169 #3	Mistras	46	892	330
25 Oct 2011	S270 #2	DWC	40	1851	305
05 Oct 2011	S322 #1	DWC	40	2946	334
15 Nov 2011	S322 #2	Mistras	46	800	352
30 Nov 2011	S322 #3	Mistras	38	15984	365

¹ Format: S (spool number) # (strand number).

² Valid failure; suspect 'infant mortality': candidates for post-mortem analysis.

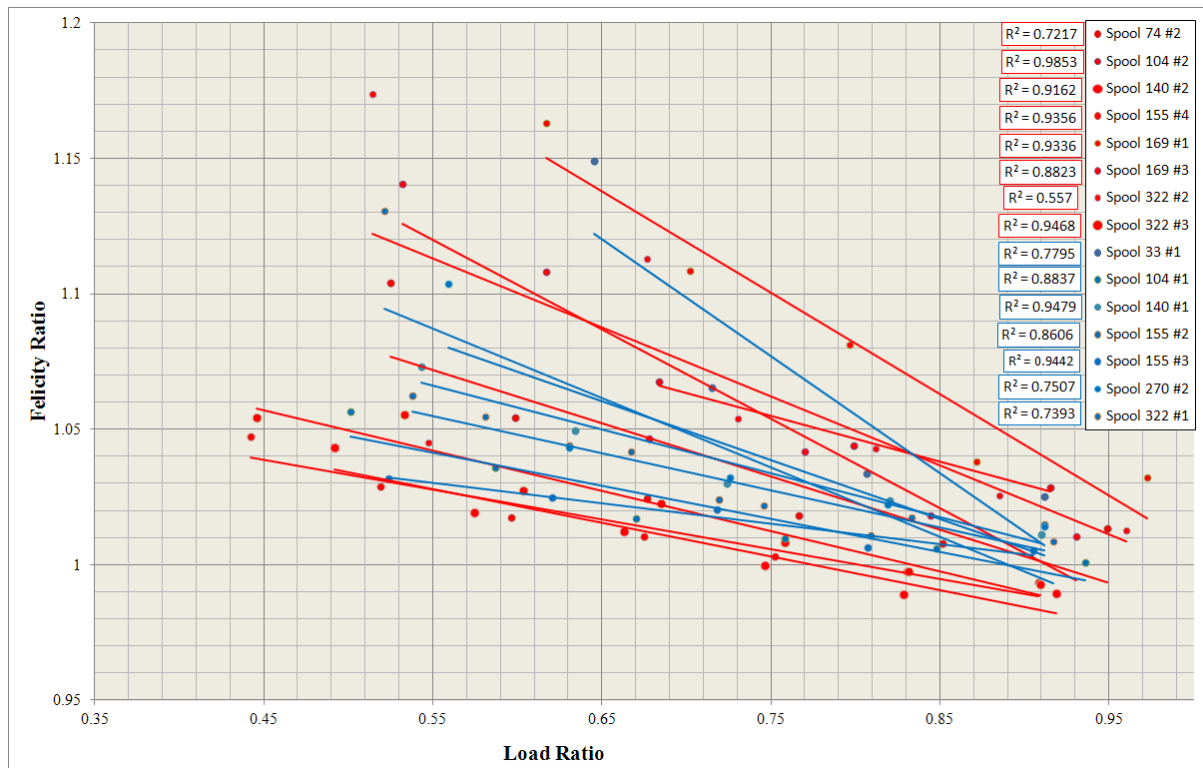


Figure 4. FR vs. LR for all tested samples. Mistras Group and Digital Wave Corporation Felicity ratio data points calculated through the exponentially weight moving average method (ignoring loading ramp 2), with in-family slopes but scatter due to acoustic emission data collection threshold differences.

E. Issues Resulting from Sparse Data

Linearity as assessed by the coefficient of determination, R^2 , in the FR versus LR plots was found highly dependent on AE data richness (Figs. 4-6). Specimens with low R^2 values often had very sparse AE data (due to the AE threshold set too high), which drastically reduced the number of AE events and especially reduced AE events in the first few loading ramps (Fig. 6). Such specimens provided poor results regardless of onset determination methods.

Conversely, the tests with the lowest thresholds and the highest numbers of AE events consistently produced FR versus LR plots with R^2 values over 0.9 (Fig. 5), which suggests low-threshold tests are desirable for better data correlation.

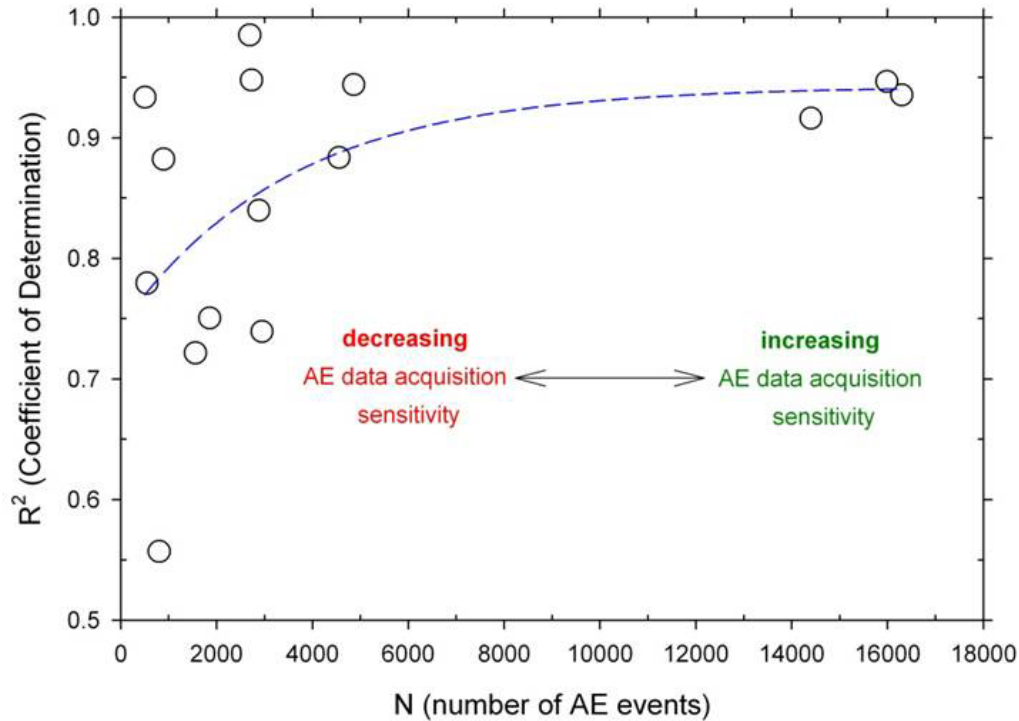


Figure 5. Effect of data richness on FR trend analysis linearity. Onset of FR determined using the EWMA2 method, showing a possible trend of increasing linearity with more AE events.

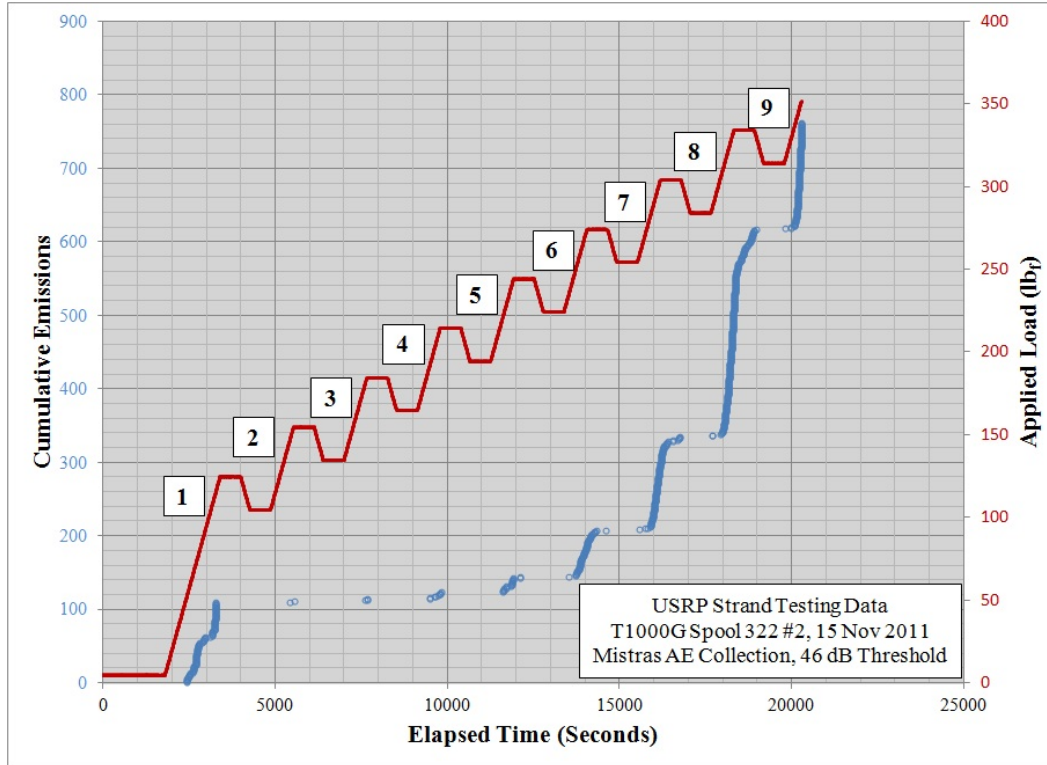


Figure 6. Sparse AE data. Sparse data (blue circles) on earlier loading ramps (red line) due to high threshold.

F. Omission of Load Ramp 2

Load ramp 2 (Fig. 6) often generates FR values that are significantly out-of-family compared to values observed during later load ramps. Inspection reveals frequent data scarcity during load ramp 2, and its inclusion in a collection of FR data points often significantly decreases the correlation between FR and LR . It is possible the ILH schedule does not stress the T1000G tow enough during load ramp 2 sufficiently to generate significant AE events, or that the initial damage mechanism operative during load ramp 2 are different from those operative during later ramps.

Accuracy improved with the omission of load ramp 2, leading to its omission in analysis for both EWMA and n-methods. This omission is the difference between EWMA1, EWMA2, and EWMA3. EWMA1 takes all available FR data points into account; EWMA2 ignores loading ramp 2; and EWMA3 ignores loading ramps 2 and 3. The methods use the same constant values, equations, and procedure for finding the onset for FR determination. Data show EWMA2 as producing the best linearity (Fig. 7).

G. Best Onset Prediction Method

Test results (Fig. 5) indicate the EWMA2 method has the highest average correlation and second lowest standard deviation of all methods, with EWMA1 having slightly lower standard deviation. The EWMA2 method currently offers the best combination of accuracy and consistency for onset determination in T1000G strands. With this established, future tests can focus on developing a statistically accurate FR^* for use with the EWMA2 method, allowing true evaluation of failure prediction. A statistically accurate FR^* will require tighter controls on spool number and AE collection parameters to ensure validity.

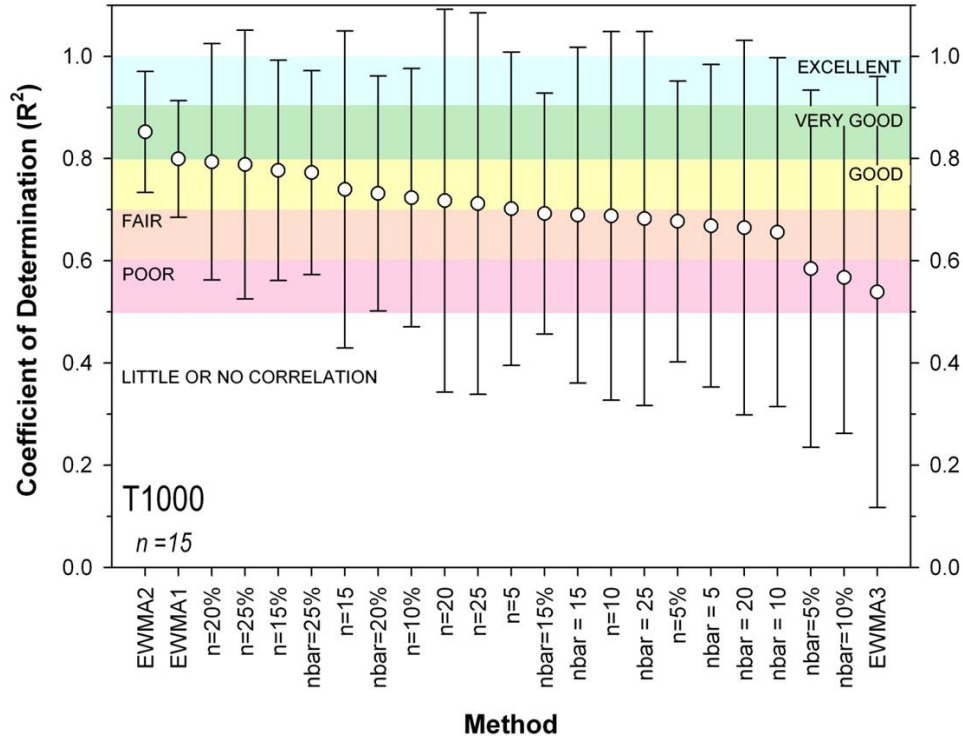


Figure 7. Method Results. Onset determination methods in order of decreasing goodness of fit (standard deviation bars shown) including averages for all 15 T1000G carbon-epoxy single tow specimens.

H. Strand Infant Mortality

Several strands tested (Table 7) fractured well below the published UTS for T1000G.¹⁹ Although isolated, these samples may be examples of the very lower end of the Weibull distribution of T1000G carbon fiber. If repeatable, these results could have serious implications towards carbon fiber usage in composite components, especially COPVs, which rely on the democratic load sharing between all the tows that are used to fabricate the overwrap to operate effectively. Unfortunately, not enough data are available from this study to evaluate the relevance of these lower breaking specimens.

V. Conclusions and Recommendations

Data show a correlation between the number of AE events collected and *FR-LR* linearity (Fig. 5). Future tests should use lower threshold settings to collect as much data as possible, relying on post-test AE data processing capabilities to determine if the correlation holds for different material types (T1000 vs. IM7), specimen geometries (tow versus laminate plate), and design (COPVs with different overwrap patterns). Lower thresholds are accompanied by a greater amount of electronic noise or artifactual events not indicative of micromechanical damage. Development of more efficient filtering methods should allow for even lower thresholds, and potentially better correlations. *FR* analysis using AE hits versus event, or different types of energy thresholds, may also result in better correlations. Regardless, this study shows that low AE data collection thresholds result in better correlation for T1000G uniaxial tow.

Application of EWMA statistical trending methods yielded more consistent correlations between *FR* and *LR* (Fig. 5) than previously developed *n*-methods. Furthermore, many EWMA parameters could be adjusted to further improve consistency and accuracy. Further testing and analysis should evaluate EWMA's performance on other materials and structures, and focus on optimizing the method's constants and parameters.

This study did not generate data to determine the underlying reasons responsible for strand infant mortality within a given population. Further testing is recommended that focuses on possible differences between the modal AE response of these specimens versus those that break in-family. Extremely serious implications arise if weak strands in turn result in weak COPVs that burst either at low accumulated life or at low pressure. To mitigate and prevent the occurrence of such scenarios, it is imperative to understand the evolution of accumulated damage in such specimens and develop AE analysis procedures that can detect such out-of-family behavior.

Acknowledgments

This work was funded by the Undergraduate Student Research Program (USRP) and the NASA NDE Working Group (NNWG). We have learned a great deal from those who have worked with us over the years and gratefully acknowledge our debt to them, especially our previous NASA Interns Daniel Wentzel, Eddie Andrade, Jon Tylka, and Doug Weathers. We would like to express our thanks to Eric Madaras (NASA-Langley Research Center), Anthony Carden (WSTF), Mike Malak (Digital Wave Corp.), as well as Ron Miller and Larry Gochbauer (Mistras) for their assistance configuring the AE test monitoring systems. Without their help, this project would not be possible. The authors also wish to thank Ben Gonzalez and Brooks Wolle (WSTF) for adding their expertise to the tests by ensuring correct tensile test procedures were followed.

References

- 1) Awerbuch, J., and Ghafari, S. "Monitoring Progression of Matrix Splitting During Fatigue Loading Through Acoustic Emission in Notched Unidirectional Graphite/Epoxy Composites," *J. Reinforced Plastics and Composites*, **7**, pp. 245-263 (1988).
- 2) de Groot, P., Wijnen, P., and Janssen, R. "Real-time Frequency Determination of Acoustic Emission for Different Fracture Mechanisms in Carbon/Epoxy Composites," *Composites Sci. Technol.*, **55**, pp. 405-421 (1995).
- 3) Shiwa, M., Carpenter, S., and Kishi, T. "Analysis of Acoustic Emission Signals Generated during the Fatigue Testing of GFRP," *J. Composite Matls.*, 30:18, pp. 2019-2041 (1996).
- 4) Ely, T. M., Hill, E. v. K. "Longitudinal Splitting and Fiber breakage Characterization in Graphite Epoxy Using Acoustic Emission Data," *Matls. Eval.*, February, 288 (1995).
- 5) Anifrani, le Floc'h, and Sornette, Souillard. "Universal Log-Periodic Correction to Renormalization Group Scaling for Stress Rupture Prediction from Acoustic Emissions," *J. Phys. I France*, **5**, 631 (1995).
- 6) Johansen, A., and Sornette, D. "Critical Ruptures," *The European Physical Journal B* 18, 163-181 (2000).
- 7) ASTM. *Standard Practice for Acoustic Emission Examination of Reinforced Thermosetting Resin Pipe (RTRP)*, ASTM E 1118, ASTM International, West Conshohocken, Pennsylvania (2000).
- 8) American Society for Nondestructive Testing, *Acoustic Emission Testing*, 3rd Ed., Columbus, Ohio (2005).
- 9) Waller, J. M., Saulsberry, R. L., and Andrade, E. "Use of Acoustic Emission to Monitor Progressive Damage Accumulation in Kevlar® 49 Composites," *QNDE Conference*, Providence, Rhode Island (July 2009).
- 10) Waller, J. M., Nichols, C. T., Wentzel, D. J., and Saulsberry, R. L. "Use of Modal Acoustic Emission to Monitor Damage Progression in Carbon Fiber/Epoxy Composites," *QNDE Conference*, San Diego, California (July 2010).
- 11) Nichols, C. T., Waller, J. M., and Saulsberry, R. L. "Use of Acoustic Emission to Monitor Progressive Damage Accumulation in Carbon Composites," *USRP Final Report*, NASA-JSC Whites Sands Test Facility, Las Cruces, New Mexico (December 2009).
- 12) Tylka J. M., Waller, J. M., Johnson, K. L., Saulsberry, R. L. "Use of Numerical Analysis of Acoustic Emission Data to Optimize Failure Prediction in Carbon-Epoxy Materials of Construction," *USRP Final Report*, NASA-JSC White Sands Test Facility, Las Cruces, New Mexico (Spring 2011).
- 13) ASTM. *Standard Practice for Acoustic Emission Examination of Fiberglass Reinforced Plastic Resin (FRP) Tanks/Vessels*, ASTM E 1067, ASTM International, West Conshohocken, Pennsylvania (2001).
- 14) ASTM. *Standard Practice for Determining Damage-Based Design Stress for Fiberglass Reinforced Plastic (FRP) Materials Using Acoustic Emission*, ASTM E2478-06, ASTM International, West Conshohocken, Pennsylvania (2011).
- 15.) ASTM. *Standard Test Method for Tensile Properties of Glass Fiber Strands, Yarns, and Rovings Used in Reinforced Plastics*. D 2343. American Society for Testing and Materials, West Conshohocken, Pennsylvania (2003).
- 16.) ASTM. *Standard Test Method for Determining Tensile Properties of Polymer Matrix Composite Materials*, D 3039. American Society for Testing and Materials, West Conshohocken, Pennsylvania (2007).
- 17) Royal Adhesives and Sealants, LLC. "Technical Information: Hardman® Extra-Fast Setting Epoxy, Double/Bubble® Red Package #04001," Belleville, New Jersey.

-
- 18) Minitab. "Technical Support Document: Unbiasing Constants c4 c5 d2 d3 d4." (July 2008) URL:
<http://mintab.com/support/documentation/Answers/UnbiasingConstantsc4c5d2d3d4.pdf> (accessed 1/8/2012).
- 19) Toray Carbon Fibers America, Inc. "Torayca® T1000G Technical Data Sheet No. CFA-008," Santa Ana, California.